JOURNAL OF SPACECRAFT AND ROCKETS
Vol. 37, No. 3, May–June 2000

Probabilistic Structural Analysis of Solid Rocket Booster Aft Skirt External Fitting Modification

John S. Townsend* and Jeff Peck*
NASA Marshall Space Flight Center, Huntsville, Alabama 35812
and
Samuel Ayala†
Sverdrup Technology, Inc., Huntsville, Alabama 35806

NASA has funded several major programs (the Probabilistic Structural Analysis Methods Project is an example) to develop probabilistic structural analysis methods and tools for engineers to apply in the design and assessment of aerospace hardware. A probabilistic finite element software code, known as NESSUS, is used to determine the reliability of a critical weld of the Space Shuttle solid rocket booster aft skirt. An external bracket modification to the aft skirt provides a comparison basis for examining the details of the probabilistic analysis and its contributions to the design process. Also, analysis findings are compared with measured Space Shuttle flight data.

Nomenclature

My = bending moment about the y axis
P_f = probability of failure
P_i^n = load on holddown post n in i direction, where $n = 5$–8 and $i = x, y, z$
x_j = random variable j
α = Weibull distribution scale parameter
β = Weibull distribution shape parameter
γ = Weibull distribution x-axis location parameter
μ = mean
σ = standard deviation
σ_j = standard deviation of random variable j

Introduction

PROBABILISTIC structural analysis has been a major research interest at NASA since 1984, with the inception of the probabilistic structural analysis methods project.[1] Designing to reliability has always been the primary goal, and developing the design tools for application and assessment of aerospace hardware has been the focus. One software tool that shows great promise is NESSUS, a probabilistic finite element program. A shortcoming of the tool is that it does not interface the probabilistic package [identified as fast probability integration (FPI)] with established finite element codes used within the industry. Making the code more usable has been a major driver. In 1995, a link between NESSUS and MSC/NASTRAN was developed that allows a NASTRAN finite element model to be analyzed probabilistically using the NESSUS FPI routines.[2] This paper details a probabilistic structural analysis of the solid rocket booster (SRB) aft skirt external fitting modification using the MSC/NASTRAN link software.[3]

This paper begins with a synopsis on the problem history of the aft skirt. It then examines details of the STS flight database, analytical and empirical models, and basics of the probabilistic analysis process. Also, the analysis effects of distribution types, random variable correlation, and curve-fitting approximations are discussed. Probabilistic analysis details of the aft skirt with and without the external bracket are presented. The paper concludes with a summary of the key study findings.

Overview

In December 1986 following the Challenger accident, a critical weld of the aft skirt failed during a qualification design test of an SRB composite case (STA-2B). The aft skirt was part of the test fixture used to apply and react the mobile launch platform (MLP) post loads defining the Space Shuttle main engine (SSME) buildup phase of launch. Maximum loading occurs ≈5 s after SSME ignition and just prior to SRB ignition and liftoff. Figure 1 shows the STS launch configuration. Note that SSME thrust forces vector off of the SRB centerline, resulting in vehicle tilting and a moment load that is reacted by the aft skirt holddown locations (four per SRB). The bending moment results in high-tension forces on the aft skirt welds of the compression posts (two per aft skirt). During the tests, the critical weld failed at a 1.28 factor of safety against the 1.4 design requirement. The failure was identified as a 28-in. (71.12-cm) crack along the weld seam of the aft skirt skin and holddown post (HDP) forging.[4] Although several design changes were implemented, each attempt failed to increase the safety factor above 1.28. The STS flights continued with a waiver signed against the 1.4 design requirement.

Recently, the aft skirt HDP region has been modified with an external bracket design (see Fig. 2). Qualification tests show the weld safety factor to be above the 1.4 design requirement. The first STS launch with the new bracket occurred in November 1998 (STS-95). After 12 years, the aft skirt weld safety issue appears to be resolved. The intent of this paper is not to redesign the new bracket using a reliability approach, but to use this problem to show what insight might occur if a probabilistic analysis is attempted. The aft skirt was the best choice of problem example simply because the authors are most familiar with its entire history and model development.

STS Flight Data

The reaction forces at the Space Shuttle vehicle/MLP interface measured during the SSME buildup phase of launch and the corresponding SRB aft skirt measured strains compose the as-measured database used in this study. Details of the MLP support post (HDP) load measurement technique are given in Ref. 4. Study findings indicated an as-measured load error of 5% axial (x) and 15% lateral (y and z). Later work determined that these inaccuracies resulted from moment loads introduced by spherical bearing frictional forces at the MLP/aft skirt boundary. Because the HDP load cells were not calibrated for moment, the as-measured loads include uncertainties due to moment effects. These loads are known to be conservative with respect to the critical weld, that is, moment loads help reduce weld strains.

Presented as Paper 99-1577 at the AIAA/ASME/ASCE/AHS/ASC 40th Structures, Structural Dynamics, and Materials Conference, St. Louis, MO, 12–15 April 1999; received 25 August 1999; revision received 7 February 2000; accepted for publication 20 February 2000.

*Aerospace Engineer, Structures, Mechanics, and Thermal Department, Engineering Directorate, ED21. Member AIAA.
†Senior Engineer II, Structures and Dynamics Group.

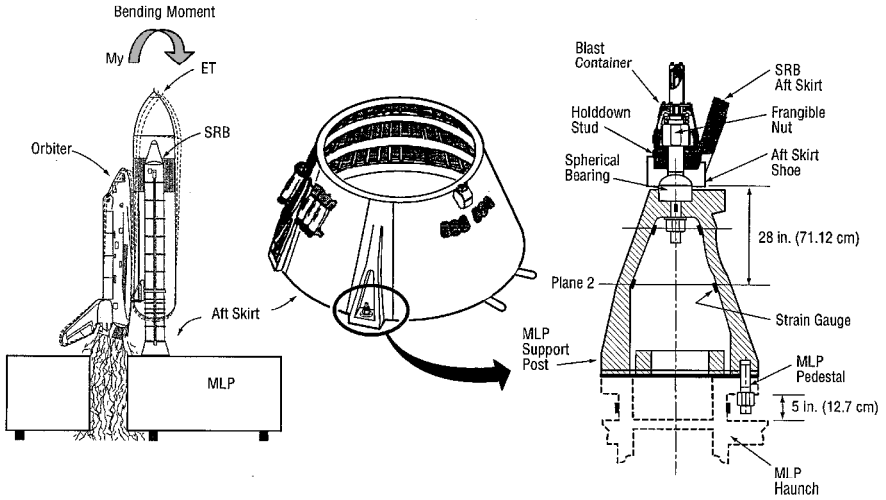

Fig. 1 Space Shuttle/SRB aft skirt/MLP HDP breakdown and preliftoff side view during the SSME buildup phase of launch.

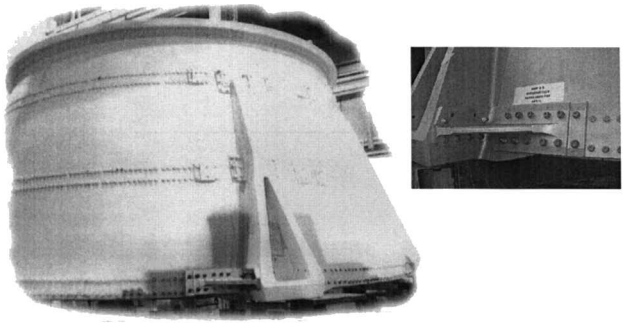

Fig. 2 Photograph of external fitting mounted to aft skirt.

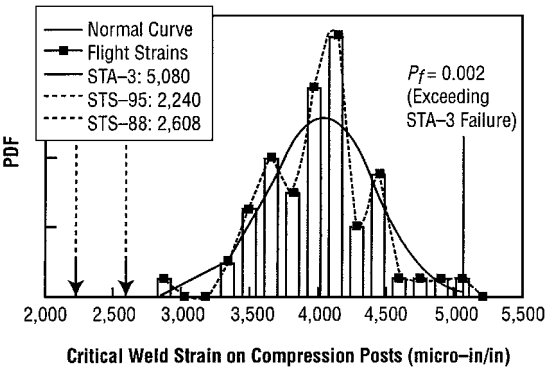

Fig. 4 PDF of aft skirt flight strains vs normal curve fit, no external fitting.

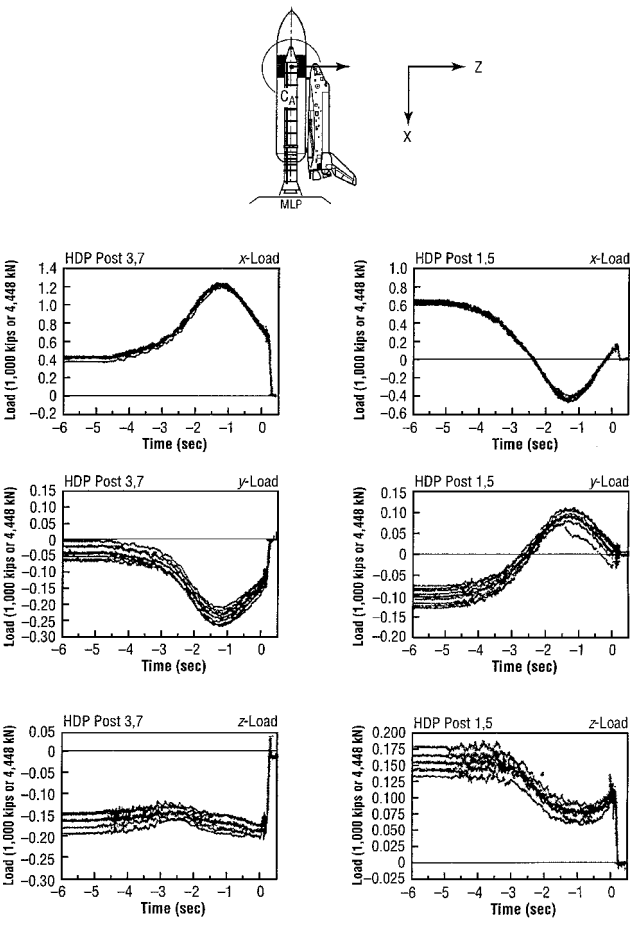

Fig. 3 HDP as-measured load histories.

Typical load histories of the SSME buildup phase are shown in Fig. 3. Notice that vertical load deviations are small, percentagewise. The horizontal loads, however, deviate significantly from flight to flight. The data scatter includes both STS flight load variations and HDP load cell measurement errors. Table 1 gives a partial listing of the maximum HDP loads measured for Space Shuttle flights STS-26 through STS-94 (25 flights). The database size was increased to 100 load sets by taking advantage of configuration symmetry (i.e., two SRBs or measured load sets per Shuttle flight) and by selecting two critical sets of time-consistent post loads per Shuttle flight. The first critical load set was chosen based on the maximum critical weld stress indicator (CWSI) [see Eq. (4)]. The second load set corresponded to the time of the peak x load value, post four of the right SRB or post eight of the left SRB. Both critical load sets occurred very near each other on the timescale. Statistical means, standard deviations (STDEVs), best-fit distributions, and correlation values of the x, y, and z as-measured loads for the left SRB (HDP 5–8) are shown in Tables 1 and 2. The tension posts are HDP five and six, whereas the compression posts are HDP seven and eight.

Figure 4 presents the summary of the as-measured aft skirt flight strains plotted as a histogram and overlaid with the associated normal (or Gaussian) probability density function (PDF). In this case, failure is defined as failure to achieve a 1.28 factor of safety as determined during the STA-3 qualification test. Based on the measured flight data, there is a 1 in 500 chance of exceeding the 5080 micro in./in. STA-3 strain value. Note that the PDF curve defines STS flights without the external bracket. To date, only two launches have occurred with the new bracket design, STS-95 and STS-88. The peak critical weld strains for both flights have been less than 2700 micro in./in.

Analysis Tools

Aft Skirt Structural Description

The SRB aft skirt is constructed primarily of 2219-T87 aluminum. Each skirt has a total of four HDP forgings, which are welded to the

Table 1 As-measured MLP HDP loads (kips)[a]

Flight	Time	Control	Pad 5x	Pad 5y	Pad 5z	Pad 6x	Pad 6y	Pad 6z	Pad 7x	Pad 7y	Pad 7z	Pad 8x	Pad 8y	Pad 8z
STS-26	5.28	Max Fx-8	−448.8	−114.5	81.2	−342.0	180.4	167.9	1225.0	224.2	−182.0	1282.4	−245.0	−141.6
STS-27	5.28	Max Fx-4	−441.1	−54.3	67.8	−348.1	135.2	154.4	1197.1	232.2	−141.7	1330.1	−302.0	−181.1
STS-29	5.31	Max Fx-4	−462.1	−111.1	73.9	−373.7	194.9	142.7	1189.0	215.0	−147.5	1327.1	−247.1	−145.7
STS-30	5.26	Max Fx-4	−433.3	−96.4	87.1	−342.4	155.6	204.0	1203.0	262.8	−184.1	1345.9	−308.3	−170.0
STS-31	5.30	Max Fx-4	−438.2	−97.1	90.6	−394.6	170.6	135.5	1239.8	235.8	−159.9	1308.9	−290.5	−164.5
STS-32	5.27	Max Fx-4	−415.0	−98.1	90.8	−277.3	166.4	182.5	1212.9	286.7	−176.0	1356.9	−333.7	−171.9
STS-33	5.38	Max Fx-4	−415.4	−100.8	74.0	−394.5	170.9	120.0	1220.3	227.9	−154.4	1333.4	−311.3	−176.0
						⋮								
STS-82	5.21	Max CWSI-8	−417.5	−84.0	96.6	−377.1	144.2	151.3	1199.2	230.3	−173.9	1332.8	−289.5	−183.2
STS-83	5.26	Max CWSI-4	−412.7	−84.8	95.9	−430.4	176.5	133.3	1223.4	233.0	−174.2	1330.8	−284.7	−169.5
STS-84	5.26	Max CWSI-8	−434.6	−61.9	93.8	−400.6	140.2	147.7	1199.8	271.5	−169.4	1304.6	−295.6	−165.2
STS-85	5.28	Max CWSI-4	−429.3	−81.0	90.6	−403.7	154.9	146.9	1196.7	249.2	−170.3	1324.8	−300.8	−170.6
STS-86	5.25	Max CWSI-8	−436.3	−77.4	90.0	−408.2	145.1	143.2	1203.7	272.8	−163.6	1307.1	−290.1	−170.1
STS-87	5.37	Max CWSI-8	−418.5	−84.4	89.3	−371.0	156.0	153.2	1199.5	232.6	−171.5	1300.1	−290.0	−179.4
STS-94	5.21	Max CWSI-8	−418.6	−87.9	83.8	−349.3	150.8	161.0	1210.0	232.0	−168.1	1280.0	−279.1	−187.9
Statistics														
Average	5.28	——	−421.7	−82.1	90.0	−375.9	155.1	149.9	1202.7	247.6	−165.8	1312.7	−290.1	−171.3
STDEV	0.07	——	20.0	15.3	10.5	28.6	17.6	13.9	20.9	17.0	13.3	24.6	17.5	12.1
Distribution	——	——	EVD[b]	N[c]	WB[d]	EVD	N	LN[e]	N	LN	EVD	LN	N	EVD

[a]Load, 1 kip × 4.448 = load, kN. [b]Extreme value. [c]Normal. [d]Weibull. [e]Log normal.

Table 2 Correlation matrix for as-measured loads[a]

Load	Pad 5x	Pad 5y	Pad 5z	Pad 6x	Pad 6y	Pad 6z	Pad 7x	Pad 7y	Pad 7z	Pad 8x	Pad 8y	Pad 8z
Pad 5x	1	——	——	——	——	——	——	——	——	——	——	——
Pad 5y	0.136	1	——	——	——	——	——	——	——	——	——	——
Pad 5z	0.481	−0.186	1	——	——	——	——	——	——	——	——	——
Pad 6x	−0.03	−0.082	−0.198	1	——	——	——	——	——	——	——	——
Pad 6y	0.111	−0.843	0.267	−0.016	1	——	——	——	——	——	——	——
Pad 6z	−0.302	−0.134	−0.145	0.565	−0.147	1	——	——	——	——	——	——
Pad 7x	−0.011	−0.254	0.328	−0.328	0.26	−0.307	1	——	——	——	——	——
Pad 7y	−0.07	0.479	−0.134	0.028	−0.498	0.167	−0.066	1	——	——	——	——
Pad 7z	−0.24	0.266	−0.445	0.176	−0.206	−0.108	−0.411	0.124	1	——	——	——
Pad 8x	0.061	−0.165	0.01	0.166	0.264	0.119	0.039	0.051	−0.122	1	——	——
Pad 8y	−0.216	−0.184	−0.053	−0.1	0.118	−0.004	−0.143	−0.564	0.043	−0.591	1	——
Pad 8z	−0.22	0.041	−0.209	0.025	−0.072	−0.139	0.138	0.088	0.312	−0.349	0.252	1

[a]Load, 1 kip × 4.448 = load, kN.

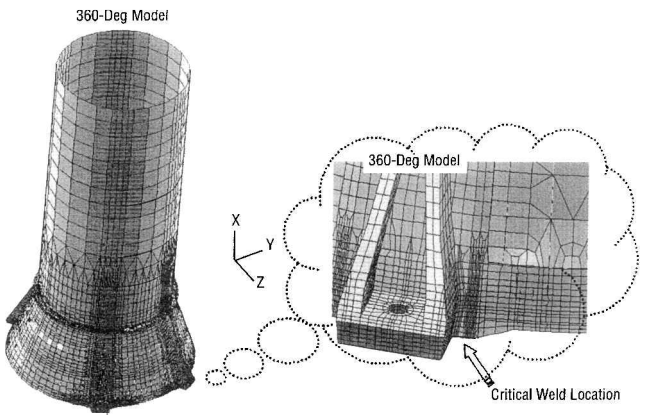

Fig. 5 NASTRAN 360-deg finite element model including SRB motor case and aft skirt.

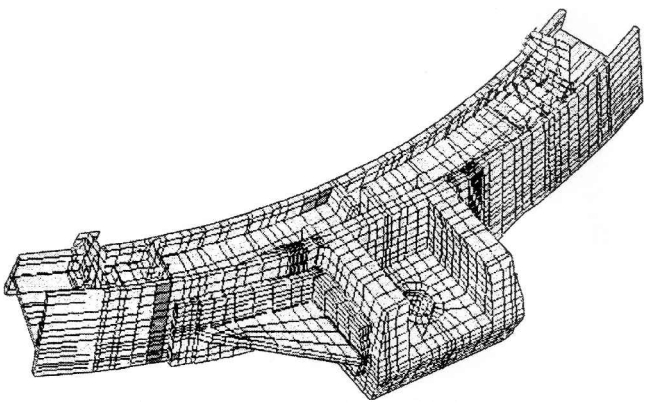

Fig. 6 Aft ring submodel including holddown post and external fitting.

skin panels (see Figs. 1, 2, and 5). A butt-weld configuration is used; the weld is ≈1.375 in. (3.493 cm) in thickness and runs the full skirt height. The highest stressed weld region occurs near the bottom of the skirt where the forging post is bolted to the MLP HDP. These HDP's react launch pad loads from the stacking operations through liftoff. Two previous static test articles were subjected to operational loads. Both articles failed at the same HDP weld location at less than the predicted failure load. Typical allowables for the skin-to-forging weld region are approximately 30.5 ksi (210.27 MN/m^2) for yield and 43.9 ksi (302.65 MN/m^2) for ultimate.

The aft skirt development test program was undertaken to evaluate a modification of the aft skirt that would alleviate the negative margin of safety concern at the welded connection of the skin to the HDP forging. An external bracket was developed that provides an additional load path from the skin to the forging and decreases the bending portion of the load carried through the weld (Fig. 6). The external bracket is manufactured from a 2219 aluminum forging. Basically, it is an angle section with one flange tied to the HDP forging side wall and the other flange spanning the critical skin-to-HDP weld. An integral gusset ties the flanges together for added stiffness (see Figs. 2 and 6). The flange on the skin side is stepped down in thickness from 1.7 to 1.13 in. (4.32 to 2.87 cm) at the last row of fasteners to smooth out the load distribution in the fasteners. A total of 11, 0.5-in.- (1.27-cm-) diam MP-35 bolts and 9, 0.5625-in.- (1.429-cm-) diam MP-35 bolts are used to attach the bracket to the skirt. The four lower bolts, which attach the external fitting to the HDP forging side wall, are held in place with floating

barrel nuts. Four 0.88-in.-(2.235-cm-) diam holes were drilled in the HDP foot pad to install these barrel nuts. The analyses summarized in this report were performed both with and without the external fitting installed.

NASTRAN Model Description

The NASTRAN model used in this analysis consisted of three major segments. The first was the G10 model, which included the total aft skirt structure plus a segment of the aft motor case. The second was a detailed submodel of a 60-deg segment of the aft ring, including the critical HDP (see Fig. 6). The third was a detailed model of the external bracket, including attachment hardware. The total model was constructed using CQUAD4 and CTRIA3 plate elements to represent the bulk of the structure that is, the aft motor case and most of the aft skirt structure (see Fig. 5). In addition, CHEXA, CPENTA, and CTETRA solid elements were used to model the detailed aft ring and HDP segments. The fasteners in the detailed submodel were represented with CELAS, RBE2, and CONROD elements.

The original NASTRAN model was a 180-deg symmetric model. The loading on the aft skirt, however, is not symmetric. A procedure was introduced that involved the application of symmetric and antisymmetric loads and boundary conditions. The resulting loads and stresses were then combined within NASTRAN using the subcom option. To simplify the process, a full 360-deg model was created by mirroring the existing 180-deg model. This change greatly simplified the script needed to drive NASTRAN, which automated the modification of random variables during the NESSUS probabilistic analysis. The resulting model contains 66,122 nodes and 51,220 elements. This size model was considered a good test of the NESSUS/NASTRAN interface software.

The model calculates the maximum von Mises stress at a single element node. Critical loads on the SRB aft skirt develop just prior to liftoff during the 7-s interval when the SSMEs are building up to maximum thrust. For analysis purposes, the model was constrained at the forward end of the aft motor case segment using a full six-degree-of-freedom constraint. The loads were applied to the aft end of the skirt post where the skirt attaches to the MLP. Applying reaction loading in this manner is the accepted method.

Load Cases

The analysis was completed using two primary sets of loads. The first set was based on actual launch pad measurements, and the second set was a nominal and worst-case design set of loads. The HDP loads represent a combination of loads due to SSME buildup, vehicle gravity loads, wind loads, mismatch loads between the aft skirt and MLP, and, finally, bias loads. Note that mismatch loads occur during the SRB aft segment setdown process of the assembly phase. Also, bias loads occur during the setdown phase due to a preload on the skirt induced by positioning the spherical bearings of the MLP HDPs inward from a perfect no-mismatch condition. As mentioned earlier, all analysis runs were completed with and without the external bracket design included in the NASTRAN model. This comparison provided a basis for examining the effects of probabilistic assumptions on analysis findings.

As-Measured Load Case

Table 1 contains the loads applied to the NASTRAN model for the as-measured load case in the orbiter global Cartesian coordinate system. Statistical data include means, STDEVs, and best-fit distributions. Table 2 is the correlation matrix that was used during the probabilistic analysis. The correlation matrix was calculated using the built-in correlation data analysis function in Excel. The correlation coefficients, which compose the matrix, are an indication of the linear relationship between random variable components. The values of the coefficients must lie in the range between -1 and 1. Absolute values close to 1 represent tightly correlated data, whereas uncorrelated data yield values close to 0. Load correlation effects on probabilistic analysis results are a primary concern in structural engineering applications where substructure loads tend to be highly correlated.

Three probabilistic analysis load cases were examined for the as-measured loads. Case 1 considered the complete probabilistic format, including load data correlation information and best-fit distributions. Case 2 was defined using best-fit distribution data, without load correlation effects considered. Case 3 assumed all distributions were normal using the means and STDEVs in Table 1. Also, case 3 load data were assumed uncorrelated.

Design Load Case

Table 3 contains a listing of two sets of loads. Case 1 defines the design case including the external bracket design with a no-bias condition. Although case 2 is a similar load set, it does not include the external bracket design. Case 2 does, however, include bias. To help clarify the load differences in these cases to the reader, the following explanation is given. The bias configuration was an attempt to improve the aft skirt weld strains without modifying the skirt structure. Although the technique did improve the weld crack safety factor to a consistent 1.28 value, it did not eliminate the engineering concerns at the weld due to material yielding. The new external bracket design improves the weld safety factor above the 1.4 design requirement with margin to spare. Thus, the bias process is no longer required and has been eliminated from the booster assembly phase. In addition, because the bracket is only applied to one side of the aft skirt posts, the MLP HDP loads are expected to be unchanged.

Analysis for the design load case was handled differently than the as-measured loads. For the design load case, the loads were broken up into their constituent components, and random variables were defined for each component load, resulting in 48 random variables vs only 12 for all as-measured analyses. This analysis provided the relative sensitivity of the various load components with respect to the stress at the critical weld location (see Fig. 5). The loads were broken up into the following components: SSME buildup load, gravity load, mismatch load, and wind load. The loads were also separated according to their components in the global Cartesian coordinate system, that is, x, y, and z.

For the design case, only limited load distribution data were available; hence, it was not possible to calculate a best-fit distribution for the data and a correlation matrix. Normal distributions were assumed for all load random variables. The significance of distribution choice on the analysis results is examined in the next section. Statistics of the design load set for each post are given in Table 3, in terms of mean and STDEV load estimates. Mismatch estimates were based on both analysis and measured data.

Probabilistic Analysis Results

The NESSUS probabilistic structural analysis program was used to complete the probability study. The 360-deg finite element model of the SRB aft skirt (see Fig. 5) was chosen as a good candidate to test the NESSUS code on a large-scale structure. The input to the NESSUS software includes the mean values for all random variables, along with their STDEVs and distribution types. A normal distribution was used in the design analysis case. For the as-measured load case, a best-fit distribution was determined for each random variable. The HDP component reactions x, y, and z at all four posts were the random variables used in this study. All other parameters such as material properties, geometry, and boundary conditions were assumed to remain fixed at their design values.

The interface between NESSUS and NASTRAN consists of custom FORTRAN code and UNIX shell scripts that allow NESSUS to perform probabilistic analyses using NASTRAN models. This code enables NESSUS to modify NASTRAN input decks, execute NASTRAN with the modified decks, and extract results from f06 files. NESSUS uses these capabilities to estimate probabilities using algorithms developed to minimize the number of functional evaluations (NASTRAN runs) required. The details of these algorithms are well documented and will not be explored here; the interested reader is directed to Refs. 5–7.

Material Properties

The aft skirt weld material properties are based on as-built coupon test data. The statistics of these material tests are given in Table 4.

Table 3 Design load cases[a]

Random variable	Post 5 Mean (kips)	Post 5 STDEV	Post 6 Mean (kips)	Post 6 STDEV	Post 7 Mean (kips)	Post 7 STDEV	Post 8 Mean (kips)	Post 8 STDEV
				With bracket, no bias				
SSME	−1007.18	13.08	−1093.67	3.98	807.59	7.63	735.67	14.93
Gravity	584.23	6.39	771.3	7.4	366.82	4.54	531.86	3.4
Mismatch	0	5.83	0	5.83	0	5.83	0	5.83
Wind	0	15.08	0	22.48	0	19.95	0	13.21
Sum x =	−422.95	——	−322.37	——	1174.41	——	1267.53	——
SSME	−279.47	2.15	327.33	2.5	200.34	0.78	−233.67	3.9
Gravity	125.69	2.06	−139.51	2.1	45.03	1.47	−58.24	1.2
Mismatch	0	9.68	0	9.68	0	9.68	0	9.68
Wind	0	4.23	0	6.43	0	4.09	0	4.42
Sum y =	−153.78	——	187.82	——	245.37	——	−291.91	——
SSME	−90.53	3.2	−95.74	1.33	−31.76	1.39	29.48	2.22
Gravity	151.43	0.27	225.42	0.69	−156.78	0.29	−219.99	0.67
Mismatch	0	2.11	0	2.11	0	2.11	0	2.11
Wind	0	0.88	0	2.58	0	2.71	0	0.64
Sum z =	60.9	——	129.68	——	−188.54	——	−190.51	——
				No bracket, with bias				
SSME	−1007.18	13.06	−1093.67	3.98	807.59	7.63	735.67	14.93
Gravity	584.23	6.39	771.3	7.4	366.82	4.54	531.86	3.4
Mismatch	0	5.83	0	5.83	0	5.83	0	5.83
Wind	0	15.08	0	22.48	0	19.95	0	13.21
Bias	0	0	0	0	0	0	0	0
Sum x =	−422.95	——	−322.37	——	1174.41	——	1267.53	——
SSME	−279.47	2.15	327.33	2.5	200.34	0.78	−233.67	3.9
Gravity	125.69	2.06	−139.51	2.1	45.03	1.47	−58.24	1.2
Mismatch	0	9.68	0	9.68	0	9.68	0	9.68
Wind	0	4.23	0	6.43	0	4.09	0	4.42
Bias	5	0	−5	0	5	0	−5	0
Sum y =	−148.78	——	182.82	——	250.37	——	−296.91	——
SSME	−90.53	3.2	−95.74	1.33	−31.76	1.39	29.48	2.22
Gravity	151.43	0.27	225.42	0.69	−156.78	0.29	−219.99	0.67
Mismatch	0	2.11	0	2.11	0	2.11	0	2.11
Wind	0	0.88	0	2.58	0	2.71	0	0.64
Bias	8.66	0	8.66	0	−8.66	0	−8.66	0
Sum z =	69.56	——	138.34	——	−197.2	——	−199.17	——

[a]Load, 1 kip × 4.448 = load, kN.

Table 4 Weld material properties[a]

Property	Yield, ksi	Ultimate, ksi
Mean μ	35.5	50
STDEV σ	1.97	2.39
A basis[b] (minimum)	30.5	43.9
B basis[c] (minimum)	32.6	46.6

[a]Stress, 1 ksi × 6.894 = stress, MN/m^2.
[b]Definition: 99% probability with 95% confidence for $N = 250$, $K = 2.542$ for normal distributions; A minimum for yield = 35.5 − K ∗ 1.97 A minimum for ultimate = 50.0 − K ∗ 2.39.
[c]Definition: 90% probability with 95% confidence for $N = 250$, $K = 1.431$ for normal distributions; B minimum for yield = 35.5 − K ∗ 1.97 B minimum for ultimate = 50.0 − K ∗ 2.39.

The original database published in 1975 comprises 250 samples and gives the A and B basis definitions for the K factors shown. Additional weld material tests have been completed since 1975 using coupons cut from full-scale aft skirt test articles, but the small sample size restricts the usefulness of the later data. The A basis yield properties in Table 4 were the values used in the study reported herein. Note that a normal distribution for the material weld properties is assumed. The normal cumulative density function (CDF) in equation format is given here for completeness:

$$\text{CDF}_N\text{: } F_x(x) = \frac{1}{\sqrt{2\pi}\,\sigma} \cdot \int_{-\infty}^{x} \exp\left[-\frac{1}{2}\left(\frac{x-\mu}{\sigma}\right)^2\right] dx \qquad (1)$$

NESSUS/NASTRAN Results and Curve Fits

The results for the as-measured load cases and the design load cases are presented in Tables 5 and 6, respectively. Tables 5 and 6 contain the von Mises stresses at the critical weld location, along with the corresponding probability level (identified in Table 5 under column headings stress and CDF-org, respectively). The column identified as CDF-fit corresponds to the probability level based on the Weibull or normal curve fit of the data results. Comparison cases with and without external fittings are shown. The results are presented both with and without use of the correlation matrix. Table 5 also presents the analysis for the as-measured case assuming a normal distribution for all random variables. A three-parameter Weibull distribution was used to model the data. The CDF equation is given here:

$$\text{CDF}_{\text{WB}}\text{: } F_x(x) = 1 - \exp\{-[(x-\gamma)/\alpha]^{\beta}\} \qquad (2)$$

The Weibull distribution parameters α, β, and γ are defined in Table 5 for each case study examined. Table 6 gives similar information for the design cases with and without the external bracket. In these two cases, a normal distribution gave the best fit for the analysis data. Means and STDEVs of the curve fit information are given.

Figure 7 is a graphical representation of the CDF results for the as-measured and design load cases. The actual analysis data and their best-fit curves are shown. The abscissa defines the critical weld stresses, whereas the ordinate represents the corresponding cumulative probability level. For example, in the design case without the bracket, there is a 70% chance that von Mises weld stress will be less than 30.5 ksi (210.27 MN/m^2), or there is a 30% chance that the weld will exceed its yield stress. Material yielding of the critical weld was measured during STA-3 testing. It is believed to have occurred during most of the STS flights. Eliminating weld material yielding was the primary driver for the aft skirt external bracket design. As shown in Fig. 7, the probability of failure due to exceeding the A basis minimum ultimate strength of the weld material is very low.

Table 5 Probabilistic analyses results for as-measured HDP load case

Stress,[a] ksi	CDF-org	CDF-fit	Stress,[a] ksi	CDF-org	CDF-fit
With correlation (no bracket)			*With correlation (with bracket)*		
33.47	10	9.309	24.145	10	9.653
34.161	20	20.987	24.6	20	20.337
35.154	40	40.142	25.24	40	39.716
35.639	50	49.316	25.579	50	50.634
38.29	85	85.089	26.152	68	67.745
38.998	90	90.097	26.634	80	79.389
40.102	95	95.093	27.291	90	90.261
40.853	97	97.085	28.036	96	96.605
47.191	99.999	99.990	29.85	99.7	99.901
			32.992	99.999	100.000
α	β	γ	α	β	γ
4.0028	1.70254	32.4488	2.92963	2.30134	23.0608
No correlation (no bracket)			*No correlation (with bracket)*		
32.577	10	9.585	23.679	10	9.463
33.569	20	20.158	24.299	20	20.431
34.969	40	40.326	25.147	40	40.317
35.577	50	49.908	25.53	50	49.995
36.775	68	67.811	26.27	68	67.570
37.745	80	79.709	26.9	80	79.737
40.434	96	96.745	27.687	90	90.225
43.514	99.6	99.873	28.593	96	96.571
49.831	99.999	100.000	30.76	99.7	99.896
			34.558	99.999	100.000
α	β	γ	α	β	γ
6.63021	2.61608	29.8194	3.93396	2.45754	22.1413
Normal (no bracket)			*Normal (with bracket)*		
29.806	1	1.000	21.9	1	0.992
31.539	5	5.002	23	5	5.031
32.462	10	9.998	23.6	10	10.260
33.581	20	20.001	24	15	15.462
34.387	30	29.993	24.3	20	20.346
35.077	40	40.004	24.8	30	30.265
35.721	50	50.002	25.2	40	39.482
37.054	70	69.996	25.4	45	44.363
37.436	75	75.001	25.6	50	49.332
37.861	80	80.002	26.5	70	70.740
38.356	85	84.998	26.7	75	74.883
38.979	90	89.997	27	80	80.464
39.903	95	94.999	27.3	85	85.218
40.172	96	95.999	27.7	90	90.249
40.503	97	97.000	28.2	95	94.613
40.943	98	98.000	28.4	96	95.849
41.636	99	99.000	28.6	97	96.844
47.807	99.9999	100.000	28.9	98	97.962
			29.3	99	98.916
			33.2	99.999	100.000
μ	σ		μ	σ	
35.7209	2.54265		25.6268	1.59986	

[a]Stress, 1 ksi × 6.894 = stress, MN/m^2.

Table 6 Design HDP loadcase results

Stress,[a] ksi	CDF-org	CDF-fit	Stress,[a] ksi	CDF-org	CDF-fit
Normal (no bracket)			*Normal (with bracket)*		
26.3	1	1.088	20.4	1	1.151
27.3	5	5.242	21	5	5.194
27.8	10	9.932	21.3	10	9.629
28.5	20	20.769	21.7	20	19.164
29.3	40	39.120	22.3	40	41.093
29.7	50	49.718	22.5	50	49.617
30.5	70	70.236	23	70	70.171
31	80	80.719	23.3	80	80.308
31.6	90	89.819	23.7	90	90.040
32	94	93.827	23.9	94	93.311
32.3	96	95.927	24.1	96	95.682
32.5	97	96.973	24.2	97	96.583
33.1	99	98.871	24.6	99	98.790
36	99.999	99.999	26.3	99.999	99.998
μ	σ		μ	σ	
29.711	1.48628		22.509	0.92778	

[a]Stress, 1 ksi × 6.894 = stress, MN/m^2.

The most salient feature of Fig. 7 is the dramatic reduction in stress, which occurs when the external fittings are installed. For the three as-measured load cases (random variable correlation, no correlation, and distribution type), the differences are minimal when compared to one another and insignificant when compared to the bracket design effects. Figure 7 also shows that the design load case distributions do not match the as-measured load distributions. Also, the as-measured loads are greater than the design loads, or the design loads are the least conservative load set with respect to the critical weld. Again, study findings indicated the as-measured horizontal loads are in error by 15%. Measurement inaccuracies result from moment loads introduced by spherical bearing frictional forces at the MLP/aft skirt boundary. The HDP load cells were not calibrated for moment. However, the comparison of the as-measured load cases with and without the bracket show the relative merits of the bracket design.

The PDF graphs of the as-measured and design load cases are plotted in Fig. 8 against the PDF for the weld material data. Only those load cases with the external bracket are shown. The probability of failure numbers for the four load cases are also given. Probability of failure was defined as follows:

$$\boldsymbol{R} - \boldsymbol{S} < \mathbf{0} \tag{3}$$

where $\boldsymbol{R}$ is material capability and $\boldsymbol{S}$ is applied stress.

To solve this equation, we assume the random variables are independent. We can then integrate over the failure region to solve for failure probabilities for each case. Note that differences in the probability values are small for the as-measured load cases. Also, the lowest failure probability value is generated from the fully correlated data set using the best-fit distributions. This result can be explained by recalling that the loads at the HDP's are reaction forces that must balance the total load from the vehicle. Because of this constraint on the post loads, the variability (STDEV) of the critical weld stress is restricted because as one post load increases, others will tend to decrease. This effect is indicated by the many negative off-diagonal terms in the correlation matrix. This finding is expected and tells the designer that assuming zero correlation for reaction loads tends to be conservative. The normal distribution assumption also gives a conservative estimate for probability, that is, overpredicts failure. These findings tend to validate the probability of failure estimate for the design load case where correlation is assumed to be zero and the distribution types are assumed as normal. Note that for all design and as-measured load cases, the probability of exceeding material yield is very unlikely.

Additional Design Load Cases

Several additional load cases were run to validate the probabilistic findings. In fact, 27 different deterministic analyses were completed, one for each STS load set. The deterministic responses were then combined into a PDF curve format and compared to the PDF curve developed from the probabilistic analysis using the statistical mean load set and distributions of the 27 cases combined. The two sets corresponded almost exactly. This comparison validated the advanced mean value probabilistic integration approach of the NESSUS code vs the standard Monte Carlo method. These curves are not presented because similar curves showing the same conclusions in other studies have been published many times.

Table 7 shows four more deterministic load sets for comparing with the probabilistic design case using NESSUS. Keep in mind, the probabilistic design case assumed 48 random variables, four per post per direction (SSME, gravity, wind, and mismatch). The deterministic runs were calculated for the individual load sets shown. Case 1 defines the nominal load set for each post, determined by adding up the mean values of the design variables for each direction on each post. Case 2 defines the mean load case plus a 3-σ load case, determined by adding the 3-σ STDEVs on top of one another in a worst-on-worst (WOW) case fashion. Case 3 shows the mean load set plus a 3-σ rss value. Case 4 shows the mean values for the as-measured loads for comparison. The subcases A and B define the load sets with and without the bracket, respectively. Note that the least conservative analysis is the full-blown probabilistic analysis using the 48 random variables. The most conservative is the

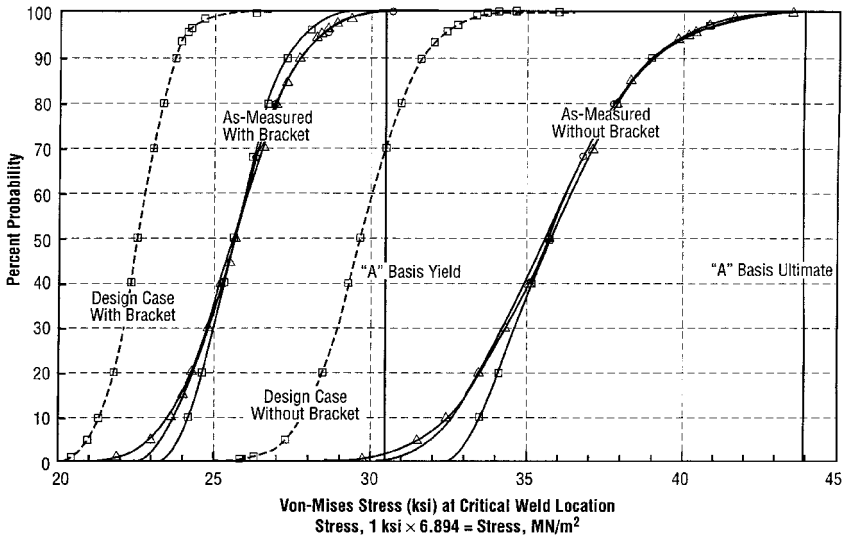

Fig. 7 CDF comparisons of aft skirt case studies with and without external bracket.

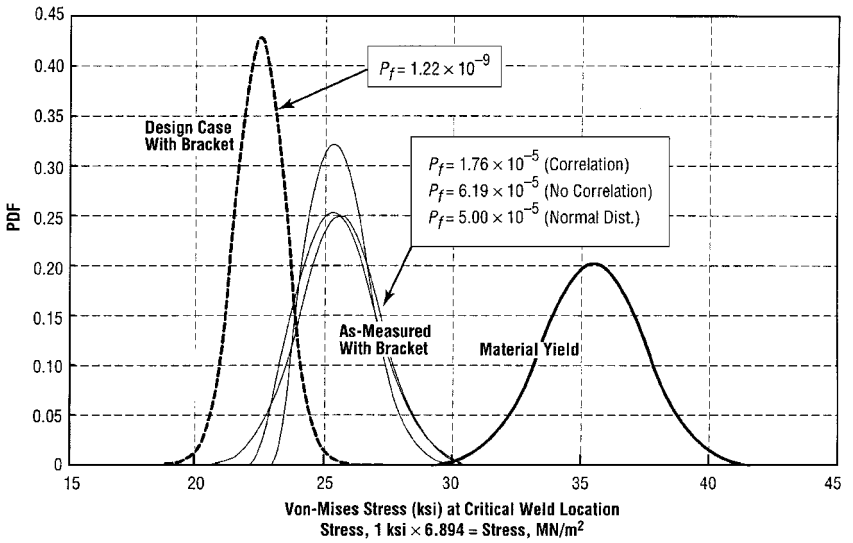

Fig. 8 PDF comparisons of aft skirt case studies with external bracket.

3-σ WOW case. The rss load set falls between the two extremes. In a safety factor design, the WOW case loads would have been multiplied by a 1.4 safety factor and used to design the bracket. Statistically, case 3, or the rss approach, offers both conservatism and merit and has recently been proposed as a possible standard.[8]

Sensitivity Analysis Results

Probabilistic Design Sensitivities

The probabilistic sensitivity data for the as-measured and design load cases are presented in Figs. 9 and 10, respectively. The response sensitivities of the random variables are plotted vs the mean post loading assumed. Both Figs. 9 and 10 are for the case with the external bracket installed. Also, the as-measured load case does not include correlation. Only absolute values were used for the sensitivities and post loads to simplify the interpretation of results. The data are separated according to load contributor, load component, and HDP number. For the design load case (Fig. 10), the load contributors are SSME loading (engine thrust), gravity loading, wind loads, and mismatch loads (between the HDP spherical bearings and the MLP posts). The chart in Fig. 10 reveals that the two largest sensitivities are the x components at HDP number 8 and result from engine thrust and wind loading. This finding is not surprising because the total x load at post 8 is the largest applied load. The post 8z components are identified as the second highest set of peaks. The z component of load corresponds to the radial direction at the HDP location. This load component contributes to the bending stress at the weld about its weak axis; hence, it is expected to be a significant contributor to the stress at the weld.

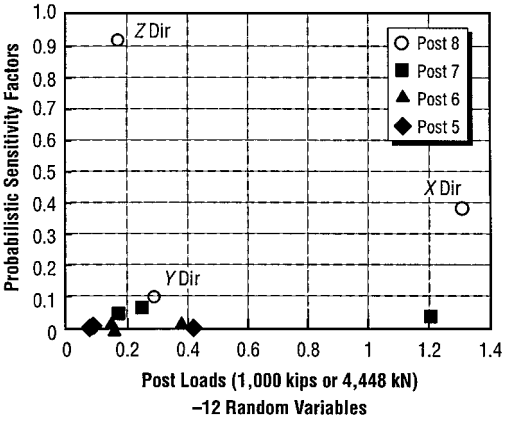

Fig. 9 As-measured load sensitivities with external fitting, no correlation.

Figure 9 of the as-measured load case shows similar findings of the dominant post 8 load sensitivities. In this case, the maximum sensitivity is in the z direction, which corresponds to the total horizontal post load (SSME, gravity, wind, mismatch, and all other loads, including uncertainties, are lumped into this single value).

Table 7 Comparison of deterministic and probabilistic design runs[a]

Case study	Post loads, kips												Von-Mises response, ksi	
	Pad 5x	Pad 6x	Pad 7x	Pad 8x	Pad 5y	Pad 6y	Pad 7y	Pad 8y	Pad 5z	Pad 6z	Pad 7z	Pad 8z	Deterministic	Probabilistic
1A[b]	−423.0	−322.4	1174.4	1267.5	−153.8	187.8	245.4	−291.9	60.9	129.7	−188.5	−190.5	22.496	22.509
2A[c]	−544.0	−441.5	1288.3	1379.6	−208.2	250.0	235.3	−291.5	41.5	117.5	−193.7	−186.9	26.379	25.292 (3σ)
3A[d]	−488.2	−396.5	1242.2	1330.7	−186.7	224.0	213.4	−257.7	49.1	118.7	−199.7	−180.9	25.740	25.292 (3σ)
4A[e]	−421.7	−375.9	1202.7	1312.7	−82.1	155.1	247.6	−290.1	90.0	149.9	−165.8	−171.3	25.628	N/A
1B[f]	−423.0	−322.4	1174.4	1267.5	−148.8	182.8	250.4	−296.9	69.6	138.3	−197.2	−199.2	29.714	29.711
2B[g]	−544.0	−441.5	1288.3	1379.6	−203.2	245.0	240.3	−296.5	50.2	126.2	−202.3	−195.6	35.502	34.169 (3σ)
3B[h]	−488.2	−396.5	1242.2	1330.7	−181.7	219.0	218.4	−262.7	57.7	127.4	−208.3	−189.6	34.982	34.169 (3σ)
4B[i]	−421.7	−375.9	1202.7	1312.7	−82.1	155.1	247.6	−290.1	90.0	149.9	−165.8	−171.3	35.721	N/A

[a]Load, 1 kip × 4.448 = load, kN; stress, 1 ksi × 6.894 = stress, MN/m^2.
[b]Nominal design loads/mean/with bracket: gravity + SSME + no wind + no mismatch + no radial bias.
[c]Design loads/mean + 3σ (WOW)/with bracket: gravity + SSME + wind + mismatch + no radial bias.
[d]Design loads/mean + 3σ (RSS)/with bracket: gravity + SSME + wind + mismatch + no radial bias.
[e]As-measured loads/mean value/with and without bias/with bracket: average of HDP loads STS-26 through STS-94.
[f]Nominal design loads/mean/no bracket: gravity + SSME + no wind + no mismatch + radial bias.
[g]Design loads/mean + 3σ (WOW)/no bracket: gravity + SSME + wind + mismatch + radial bias.
[h]Design loads/mean + 3σ (RSS)/no bracket: gravity + SSME + wind + mismatch + radial bias.
[i]As-measured loads/mean value/with and without bias/no bracket: average of HDP loads STS-26 through STS-94.

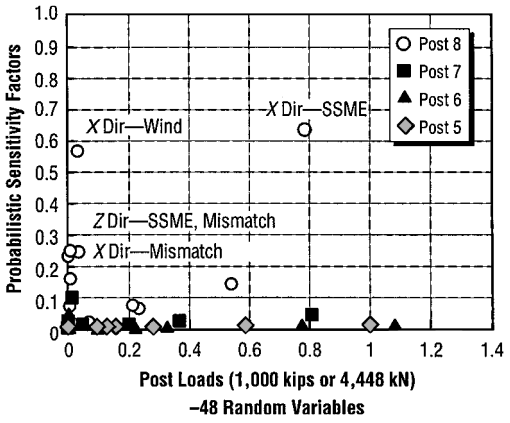

Fig. 10 Design load sensitivities with external fitting.

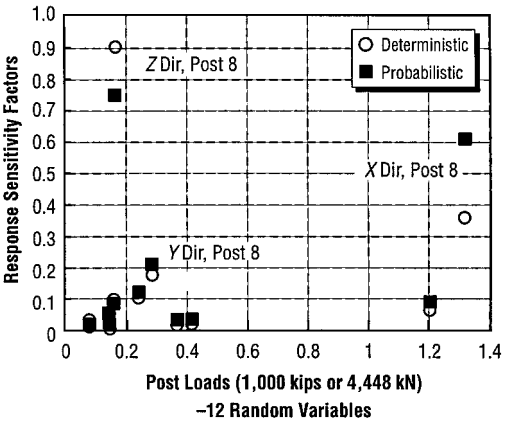

Fig. 11 Comparison of deterministic and probabilistic load sensitivities.

Again, the as-measured load set results magnify the measurement error due to moment effects.

As a final note, sensitivity studies help to determine the important variables to consider in an analysis. Obviously, it is not practical to examine all primitive variables of a given problem. Once the important drivers are identified, however, the problem can be simplified and a probabilistic analysis completed. In many applications, a simplified, closed-form equation based on a few dominant variables can be determined using "design of experiments." In this particular study, the 48 independent random variables can be reduced to a simple two-random-variable problem to estimate failure probabilities. Although these results are not presented within this paper, the findings indicate that sensitivity information can be used to significantly reduce problem complexity. The response equation data will be published at a later date.

Probabilistic vs Deterministic

To help the reader understand the differences between probabilistic and deterministic sensitivity factors, a closed-form equation is provided.[4] This equation is known as the CWSI for post 8:

$$\text{CWSI}^8 \cdot 100 = g = -0.650P_x^5 + 0.324P_y^5 + 0.921P_z^5 - 0.420P_x^6 + 0.350P_y^6 + 1.414P_z^6 + 1.90P_x^7 - 3.139P_y^7 + 3.037P_z^7 - 11P_x^8 - 5.556P_y^8 - 27.62P_z^8 \quad (4)$$

This equation was developed by USBI Company (United Technology Corp.) using both design and test information. The value calculated by this equation is not a strain or stress number, but an indicator number defining how the skirt weld strains will respond to the component post loads. The deterministic and probabilistic sensitivity equations are defined here:

$$S_{\text{Det}} = \frac{\partial g/\partial x_j}{\sqrt{\sum_{j=1}^{N}(\partial g/\partial x_j)^2}}$$

$$S_{\text{Prob}} = \frac{(\partial g/\partial x_j)\cdot\sigma_j}{\sqrt{\sum_{j=1}^{N}[(\partial g/\partial x_j)\cdot\sigma_j]^2}} \quad (5)$$

Note that the differences in these two equations involve the STDEV (σ) or uncertainties of the variables. Also, notice that both equations are normalized so that the maximum value is never greater than 1. Table 8 presents the as-measured sensitivity results for these two cases. The best-fit distribution types are given for completeness. The sensitivity results are plotted in Fig. 11. Even for this simplified model, the x and z component loads of post 8 dominate as the key parameter drivers. The deterministic and probabilistic sensitivities are very similar. The importance of uncertainties becomes apparent for these key loads. Note, the deterministic numbers identify the z-directional load to be more than twice as significant in determining CWSI as the x-directional load. However, the probabilistic sensitivities show the x and z loads to be of almost equal importance. Also, Table 8 shows that the post 8x load STDEV is about 2% of the mean value, whereas the post 8z load STDEV is about 7%. The probabilistic sensitivity number for the post 8x loads is twice the value of the deterministic sensitivity (with only a 2% uncertainty). It is important that 1) the designer be aware of the STDEV or uncertainty effects of random variables on probabilistic numbers and 2) in many design cases where parameter STDEVs are about the

Table 8 Deterministic and probabilistic sensitivity factors[a]

HDP number	Mean load kips	STDEV	Distribution type[b]	Load indicator	Deterministic sensitivity	Probabilistic sensitivity
5*x*	−421.7	20.0	EVD	−0.65	−0.0212	−0.0289
5*y*	−82.1	15.3	N	0.324	0.0106	0.0110
5*z*	90.0	10.6	WB	0.921	0.0300	0.0216
6*x*	−375.9	28.6	EVD	−0.42	−0.0137	−0.0267
6*y*	155.2	17.6	N	0.35	0.0114	0.0137
6*z*	149.9	13.9	LN	1.414	0.0461	0.0436
7*x*	1202.7	20.9	N	1.9	0.0619	0.0884
7*y*	247.6	17.0	LN	−3.139	−0.1023	−0.1190
7*z*	−165.8	13.4	EVD	3.037	0.0990	0.0902
8*x*	1312.7	24.6	LN	−11	−0.3586	−0.6025
8*y*	−290.1	17.5	N	−5.556	−0.1811	−0.2158
8*z*	−171.3	12.1	EVD	−27.62	−0.9003	−0.7457

[a]Load, 1 kip × 4.448 = load, kN.
[b]See footnotes to Table 1.

same, deterministic sensitivity analysis may be used to define the important life variables.

Conclusions

The objectives of this task were to use the NESSUS software to determine a probabilistic estimate of the reliability of the SRB aft skirt external fitting modification for both the as-measured load case and the design load case. In addition, it was necessary to obtain information on the relative sensitivity of the stress at the critical weld location to the various random variables identified. The NESSUS software enabled us to generate estimates of structural reliability and identify the important random variables with relatively few structural analyses. The results of this probabilistic analysis provided further confidence in the reliability of the external fitting modification. In addition, the results of the design load case indicate that the most significant components of load are those induced by engine thrust and wind loading. One shortcoming identified in this exercise was the limitation in the software link between NESSUS and NASTRAN, which only allows for output at a single point on the structure at a time. This area should be addressed in future versions of the code.

Several key findings that may generally be applied to probabilistic analysis are as follows:

1) The correlation effects of probabilistic load variables are not always an important factor when completing a probabilistic analysis. Also, it does not always appear necessary to complete a probabilistic design using primitive variables because for certain types of random variables (such as reaction loads) assuming independence yields a conservative estimate of reliability.

2) With respect to design reliability, the choice of the input variable distribution model does not appear as important as other factors, such as scatter, mean, and correlation.

3) Probabilistic design based on load random variables can be reasonably estimated for structures using nominal or average loads plus an rss value for the STDEVs.

4) Important probabilistic design variables can be estimated from deterministic models and an understanding of the load uncertainties.

Acknowledgment

The authors express their sincere thanks to Brian Pung, Aft Skirt Structures Manager of NASA Marshall Space Flight Center, for his efforts and guidance in completing this work.

References

[1]"Probabilistic Structures Analysis Methods for Select Space Propulsion System Components (PSAM)," NASA Contract NAS3-24389, Southwest Research Inst., Project 06-8339, March 1986.

[2]"NESSUS/NASTRAN Interface," NASA Contract NAS8-39797, Southwest Research Inst., Project 06-7212, July 1996.

[3]Townsend, J., and Smart, C., "Reliability/Risk Analyses Methods and Design Tools for Application in Space Programs," AIAA Paper 98-5276, Oct. 1999.

[4]Richardson, J., and Townsend, J., "Examining the Accuracy of the Space Shuttle Support Loads Using Probabilistic Analysis Techniques," *Journal of Spacecraft and Rockets*, Vol. 31, No. 5, 1994, pp. 814–820.

[5]Wu, Y.-T., Burnside, O. H., and Cruse, T. A., "Probabilistic Methods for Structural Response Analysis," *Proceedings of the Joint ASME/SES Applied Mechanics and Engineering Sciences Conference*, American Society of Mechanical Engineers, Fairfield, NJ, 1988.

[6]Wu, Y.-T., Millwater, H. R., and Cruse, T. A., "An Advanced Probabilistic Structural Analysis Method for Implicit Performance Functions," *Proceedings of the 30th AIAA/ASTM/AHS/ASC Structures, Structural Dynamics, and Materials Conference*, AIAA, Washington, DC, 1989, pp. 1852–1859.

[7]Madsen, H. O., Krenk, S., and Lind, N. C., *Methods of Structural Safety*, Prentice–Hall, Englewood Cliffs, NJ, 1986, pp. 44–145.

[8]Goldberg, B., and Verderaime, V., "Quasi-Static Probabilistic Structural Analyses Process and Criteria," NASA TP-209038, Jan. 1999.

R. B. Malla
Associate Editor